Transition of Subcritical Baroclinic Flows to Turbulence

A thesis Submitted
in Partial Fulfilment of the Requirements
for the Degree of

MASTER OF SCIENCE

by

Kaushal Gianchandani

to the

School of Physical Sciences

National Institute of Science Education and Research

Bhubaneswar

Date: June 28, 2022

To my parents, Shri Doulat T. Gianchandani and Shrimati Devi Gianchandani.

DECLARATION

I hereby declare that I am the sole author of this thesis in partial fulfillment of the requirements for a postgraduate degree from National Institute of Science Education and Research (NISER). I authorise NISER to lend this thesis to other institutions or individuals for the purpose of scholarly research.

Kaushal Gianchandani
Date: April 30, 2017

The thesis work reported in the thesis titled Transition of Subcritical Baroclinic Flows to Turbulence was carried out under the supervision of Dr. Antoine Venaille of ENS de Lyon and Dr. Prasanjit Samal of NISER, in the school of School of Physical Sciences at NISER, Bhubaneswar, India.

Dr. Antoine Venaille
Laboratoire de Physique
ENS de Lyon

Dr. Prasanjit Samal
School of Physical Sciences
NISER Bhubaneswar

ACKNOWLEDGEMENTS

I would first like to thank my thesis advisors Dr. Antoine Venaille of the Laboratorie de Physique, ENS Lyon and Dr. Prasanjit Samal of the School of Physical Sciences, NISER Bhubaneswar. Dr. Venaille was always available whenever I had a query regarding anything or if I ran into a trouble spot. I am grateful for all his knowledge, tireless assistance and immense patience. I would also like to acknowledge Dr. Samal as the second reader of this thesis, and I am gratefully indebted to him for his very valuable comments.

Finally, I must express my very profound gratitude to the Undergraduate Committee of the School of Physical Sciences, NISER Bhubaneswar. Without their encouragement and support, this venture would not have been successful.

ABSTRACT

We investigate the two-layer quasigeostrophic flow incorporating the effect of planetary vorticity gradient (β) to address the equilibration of meandering jets around the midlatitudes, paying particular attention to the baroclinically subcritical regime in the presence of a small bottom drag. In this regime, no turbulence is predicted to occur due to (linear) baroclinic instability. However, because of the small drag at the bottom, an instability grows in the initial stages of the flow, which eventually leads to turbulence. The flow equilibrates and we register strong nonlinear reorganisation of the flow structures into potential vorticity staircases. We quantise the various characteristics associated with the staircase and establish that the presence of such staircase like structures can be attributed to the steep meridional gradient of the Coriolis force which resulting in dominant effects of rotation. Additionally, positive feedback mechanisms and wave turbulence may also contribute to the formation and retention of these structures.

Contents

List of Figures

List of Tables

Chapter 1

Introduction

Narrow bands of strong meandering winds found in the troposphere of various planets like the Earth, Jupiter and Saturn are referred to as jet streams. The ones occurring closer to the poles are called polar jet streams. They occur at higher altitudes typically of 7 to 12 km above the Earth's surface. Jet streams correspond to the boundaries between warm air and cold air.

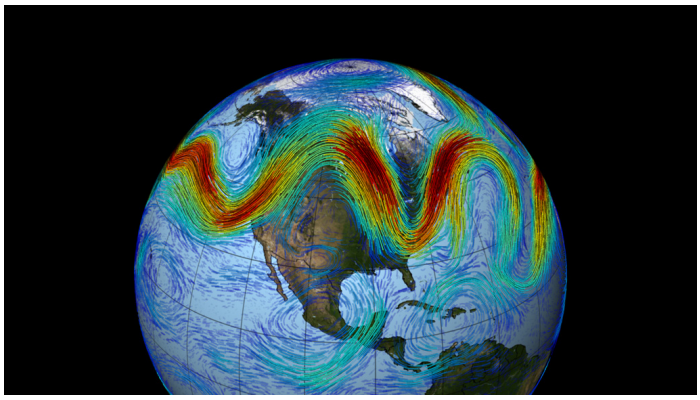

Figure 1.1: Visualisation of polar jet streams. The fastest winds are represented by red colour and the slower ones are depicted by blue colour. Source: NASA/Goddard Space Flight Center.

These winds therefore have a huge impact on the weather conditions of the midlatitude region. Due to their enormous impact on us and the planet as a whole, a lot of investigation has been carried out regarding these streams. The sharp meandering eastward jets at midlatitudes are explained well by the concept of baroclinic instability [1]. A lot of attention has been paid to the supercritical flow and the linear behaviour of the instability [2] is well understood, but the nonlinear equilibration of baroclinically steady flows [3, 4] still requires further investigation.

During this study, we aim to explore the effect of planetary vorticity gradient (β). Various studies have looked at the effect of β [5] and bottom drag [6] independently and in combination [7] as well but we believe that much needs to be explored and understood about the nonlinear equilibration of the system for large values of β (subcritical limit) in the presence of bottom friction.

In particular, we show that in presence of a small damping effect (due to bottom friction) the subcritical regime can lead to strongly nonlinear structure through which eventually leads to the formation of sharp jets and ribbon-like structures even when the flow is baroclinically stable.

Chapter 2

Baroclinic Flows

Let us consider a fluid parcel which is in hydrostatic balance i.e. the force due to pressure gradient and the action of gravity on the fluid balance each other.

$$\begin{aligned} -\frac{\nabla p}{\rho} - \nabla\Phi &= 0 \\ \implies \frac{\partial p}{\partial z} &= -\rho g \end{aligned}$$

Here p is the pressure, $\Phi = gz$ is the geo-potential, g is the gravitational acceleration and ρ is the density of the fluid.

We consider the flow for a small Rossby number. **Rossby number** is a dimensionless parameter is defined as the ratio of the intrinsic acceleration to the acceleration associated with the Coriolis force. It is given as $\frac{U}{fL}$ where U is the typical horizontal velocity, L is the typical horizontal length scale and f is the Coriolis parameter.

For small Rossby number, there is a dominant balance between the Coriolis force and the horizontal pressure gradient in the horizontal direction. This gives rise to the winds called the geostrophic winds, and the balance is known as the geostrophic balance.

$$u_g = -\frac{1}{\rho f}\frac{\partial p}{\partial y} \tag{2.1a}$$

$$v_g = \frac{1}{\rho f}\frac{\partial p}{\partial x} \tag{2.1b}$$

The combination of hydrostatic and geostrophic balance are the primary mechanism leads to thermal wind balance and these winds are the primary mechanism for jet streams.

The presence of this steady geostrophic flow indicates that a reservoir of potential energy is present. Baroclinic instability is a mechanism of extraction of energy from the reservoir of potential energy associated with tilted isopycnals. To understand the instability, we consider quasigeostrophic (QG) dynamics.

Equations describing the QG dynamics are obtained from primitive equations by considering asymptotic expansion in terms of Rossby number [8]. The lowest order term gives geostrophic balance and the flow dynamics obtained at next order in the asymptotic development is called quasi-geostrophic dynamics. Considering two layers is the easiest way to account for the stratification. The model is widely used to explain the dynamics in midlatitude regions.

2.1 Turbulence in two-layer quasi-geostrophic flows in a β channel

As has been mentioned earlier, baroclinic instability is a mechanism of extraction of energy from the mean flow in a quasi-geostrophic setting. To explore this is more detail let us consider a two-layer quasi-geostrophic model which in a β-plane. The two layers have equal depth and are spread across the dimensions $L \times L$. It should be noted that this choice of the dimensions isn't unique. A similar analysis can be carried out for a channel of any dimension $L \times W$. It is best to introduce a non-dimensional parameter the **domain aspect ratio**.

The domain aspect ratio is defined as the ratio of the length of the channel to its width. For the purpose of this study we considered it equal to unity but the properties of the flow may depend strongly on this ratio.

It was ensured that $\frac{1}{k_d} << L$, to make sure that the results obtained are consistent with the geophysical length scale. Another advantage of working in this setting was that in many cases the instability length scale is $\sim \frac{1}{k_d}$, thus making it possible to

study inverse energy cascade.

In general, QG dynamics assume $L \sim \frac{1}{k_d}$, but it is standard practice to use this model even when $L >> \frac{1}{k_d}$, to have a basic understanding of planetary dynamics.

The dynamics of the flow can be described using the following equations:

$$\partial_t q_1 + J(\Psi_1, q_1) + \beta \partial_x \Psi_1 = 0 \tag{2.2a}$$

$$\partial_t q_2 + J(\Psi_2, q_2) + \beta \partial_x \Psi_2 = 0. \tag{2.2b}$$

Here β is the gradient of the Coriolis parameter. We consider the flow to be doubly periodic, i.e. $\Psi(x, y) = \Psi(x + L, y) = \Psi(x, y + L)$. The potential vorticities can be expressed as a function of stream functions as:

$$q_1 = \nabla^2 \Psi_1 + \frac{k_d^2}{2}(\Psi_2 - \Psi_1) \tag{2.3a}$$

$$q_2 = \nabla^2 \Psi_2 + \frac{k_d^2}{2}(\Psi_1 - \Psi_2). \tag{2.3b}$$

Here, k_d is the deformation wavenumber, it is the wavenumber corresponding to the **deformation radius**.

The deformation radius is the length scale at which geostrophic balance plays significance i.e. the rotation of Earth comes into the picture. The Rossby radius of deformation is the length scale of the system, related to its stratification and rotation. It can be calculated for a given setting using the following expression:

$$\frac{1}{k_d} = \frac{\sqrt{gH}}{2f_0}. \tag{2.4}$$

where g is the gravitational attraction, H is the height of the fluid and f_0 is the Coriolis parameter.

The value of deformation radius as calculated for the Earth's ocean and atmosphere at 45° latitude are $\sim 2 \times 10^6$ m and $\sim 3 \times 10^6$ m. Before proceeding any further the parameters associated with the dynamics of the flow require some elaboration.

2.2 Adimensional parameters

2.2.1 The β-plane

The Coriolis force is the fictitious force which appears in motion due to the rotation of Earth. The Coriolis frequency f is given by:

$$f = 2\Omega \sin(\phi), \tag{2.5}$$

where Ω is the rotation rate of Earth and ϕ is the latitude of the point of observation. The parameter f varies with latitude. For a small variation in latitude, the variation can be approximated to be linear. This is known as the β-plane approximation. It is known that large values of β tend to stabilise flows in the absence of bottom drag [1].

2.2.2 Criticality ξ

The criticality of a two layer quasi-geostrophic model is defined as follows:

$$\xi = \frac{U k_d^2}{2\beta} \tag{2.6}$$

The parameter determines the linear instability for the system. For sufficiently large values of β, the classical criterion for stability is satisfied. In fact, β effect is commonly considered as a stabilising parameter [1] . However, for the nonlinear model, the instability can arise even if it is linearly stable [9]. In fact, all the flows become unstable with respect to baroclininc instability in the presence of bottom drag [6].

We targeted at investigating the effects of $\hat{\beta} = \frac{1}{\xi}$ on the flow, particularly how the dynamics of the flow evolves for large values.

2.2.3 Bottom Drag r_{ek}

The bottom drag acts as a sink of energy for the instability under consideration. The growth of the vertical velocity in the lower layer incorporates the Ekman drag. It has

been already shown that Ekman drag cannot certainly eliminate baroclinic instability [10]. Although friction can reduce the growth rate of the most unstable mode.

2.3 Evolution of a perturbation around a prescribed eastward jet

We assume that there is constant eastward flow in the upper layer whereas the lower layer is at rest. ($\bar{\Psi}_1 = -Uy$, $\bar{\Psi}_2 = 0$). If we assume that the stream function Ψ_i is given as $\Psi_i = \bar{\Psi}_1 + \psi_i$ where ψ_i is the perturbation around the prescribed flow, we can easily obtain the linearised equations:

$$(\partial_t + U\partial_x)q_1 + \beta_1\partial_x\psi_1 = 0 \tag{2.7a}$$

$$\partial_t q_2 + \beta_2\partial_x\psi_2 = 0. \tag{2.7b}$$

where

$$q_1 = \nabla^2\psi_1 + \frac{k_d^2}{2}(\psi_2 - \psi_1) \tag{2.8a}$$

$$q_2 = \nabla^2\psi_2 + \frac{k_d^2}{2}(\psi_1 - \psi_2) \tag{2.8b}$$

and

$$\beta_1 = \beta + \frac{k_d^2}{2}U \tag{2.9a}$$

$$\beta_2 = \beta - \frac{k_d^2}{2}U. \tag{2.9b}$$

Assuming $\psi_i = \Psi_i^A e^{\iota(kct-kx-ly)}$ and substituting $k_\beta = \sqrt{\frac{\beta}{U}}$, into the solution would give us the dispersion relation for the 2-layer QG model incorporating β. A similar analysis has been carried out in Reference [1].

The flow is supercritical in the domain for $\hat{\beta} < 1$ and there exists the baroclinic instability for this regime. The instability grows during the initial evolution of the flow and the flow soon becomes turbulent. The supercritical domain has been studied

extensively during the past. It's the transition from supercritical to subcritical domain which reveals certain profound novel results which have been discussed in the subsequent chapters. Before discussing this transition, it is important to account for the energy budget involved.

2.4 Energy budget

The energy of the perturbation is the sum of kinetic energy in each layer and of the available potential energy,

$$E = KE_1 + KE_2 + APE, \tag{2.10}$$

$$KE_i = \frac{1}{2}\int_D dxdy(\nabla\psi_i)^2, \tag{2.11}$$

$$APE = \frac{1}{2}\int_D dxdy(\psi_1 - \psi_2)^2 k_d^2. \tag{2.12}$$

Here KE_i is the kinetic energy of the i^{th} layer. An important diagnostic quantity associated with the kinetic energy of the flow is the growth rate. As the name suggests, the growth rate of any instability is defined as the rate at which an instability grows or the rate at which the potential energy available is converted to kinetic energy.

2.5 Baroclinic and barotropic decomposition

The barotropic and baroclinic streamfunctions are defined as:

$$\eta \equiv \frac{1}{2}(\psi_1 + \psi_2) \tag{2.13a}$$

$$\tau \equiv \frac{1}{2}(\psi_1 - \psi_2). \tag{2.13b}$$

The potential vorticities can be expressed in terms of baroclinic and barotropic modes as:

$$q_1 = \nabla^2\eta + (\nabla^2 - k_d^2)\tau \tag{2.14a}$$

$$q_2 = \nabla^2\eta - (\nabla^2 - k_d^2)\tau. \tag{2.14b}$$

and thus the equations describing the flow dynamics become:

$$\left(\partial_t \nabla^2 + U\partial_x \nabla^2 + \beta_1 \partial_x\right)\eta + \left((\nabla^2 - k_d^2)(\partial_t + U\partial_x) + \beta_1 \partial_x\right)\tau = 0 \quad (2.15a)$$

$$\left(\partial_t \nabla^2 + \beta_2 \partial_x\right)\eta - \left(\partial_t(\nabla^2 - k_d^2) + \beta_2 \partial_x\right)\tau = 0 \quad (2.15b)$$

Assuming plane wave solutions for η and τ and carrying out some simple manipulations, the adimensional growth rates for barotropic and baroclinic modes [1] can be obtained as:

$$\hat{\sigma_\eta} = \hat{k}\left[1 + \frac{1}{\hat{K}^2} + \frac{\hat{\beta}}{2(\hat{K}^2 - 1)}\right] \quad (2.16)$$

$$\hat{\sigma_\tau} = \hat{k}\left[1 + \frac{\hat{\beta} + 1}{2(\hat{K}^2 - 1)}\right]. \quad (2.17)$$

The decomposition illustrated above is important from the perspective of understanding geostrophic turbulence. We now move to finding solutions the flow equations numerically and studying the various aspects of the flow as it transitions from supercritical to subcritical domain.

Chapter 3

Numerical Results

The simulations are performed in a quasi-geostrophic setting using the Phillips model for baroclinic instability using the package `pyqg`[1]. The system of nonlinear equations describing the flow dynamics are solved by using a pseudo-spectral doubly-periodic model.

The instability is triggered by setting the potential vorticities to random initial fluctuations obtained from a uniform distribution. All the results discussed in this article are obtained from the same set of initial conditions and the corresponding potential vorticity fields q_1 and q_2 are represented on Fig. 3.1, however the results are independent of the initial conditions.

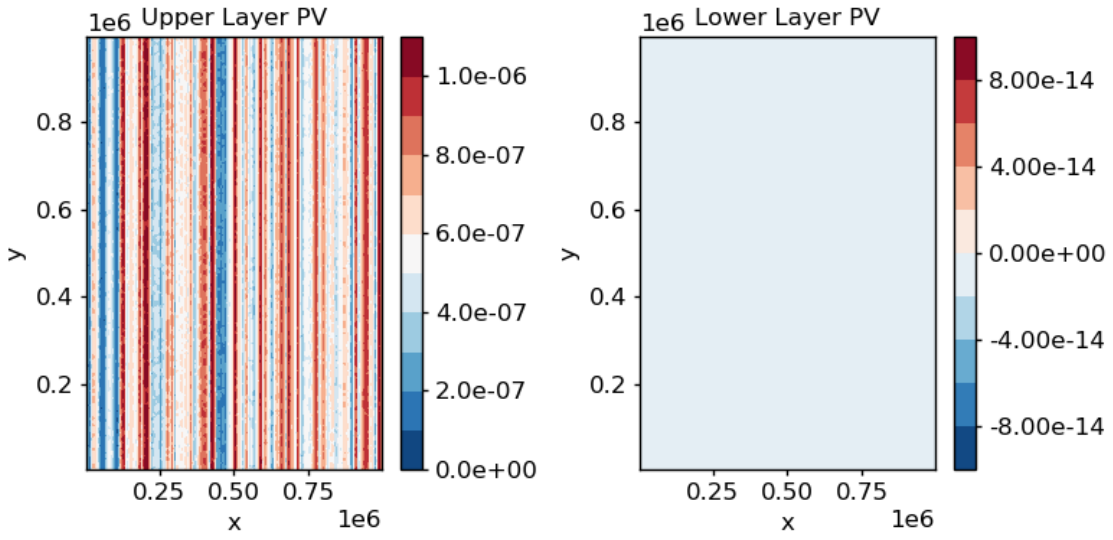

Figure 3.1: Initial potential vorticity profiles in the two layers

The non-dimensional parameters associated with the problem are — criticality

[1] `http://pyqg.readthedocs.io/en/stable/`

($\xi = \frac{Uk_d^2}{\beta}$), bottom drag ($\hat{r}_{ek} = \frac{r_{ek}}{Uk_d}$), deformation radius (set to 1), domain aspect ratio (L/W), resolution ($\Delta x/L$). The domain aspect ratio for the problem is chosen to be unity; this choice is not unique and an interesting extension of this work can be to investigate the flow dynamics for different domain aspect ratios. We also verified that the results obtained were independent of the resolution. The parameter under study - $\hat{\beta}(= 1/\xi)$ is varied from 10^{-3} to 10 and special attention is paid to the dynamics around the transition region (around $\hat{\beta} = 1$). The parameters associated with the problem are summarised in Table 3.1. All the simulations have been performed in the same configuration except when $\hat{\beta} \geq 4.0$, for these simulations we used $L_x = L_y = 2.5 \times 10^5$ m.

Parameter	Value
Imposed Velocity	$U = 0.025$ ms^{-1}
Channel length	$L_x = 10^6$ m
Channel width	$L_y = 10^6$ m
Deformation radius	$1/k_d = 15000$ m
Ratio of heights of the two layers	$\delta = 1$
Height of the upper layer	$H_1 = 500$ m
Coriolis frequency	$f = 1.0$ rad s^{-1}
Bottom drag	$\hat{r}_{ek} = 0.01$
Horizontal resolution	$\Delta x = \Delta y = L_x/128$
Planetary vorticity gradient	$\hat{\beta}$ from 10^{-4} to 10

Table 3.1: Model parameter for the simulations. All the simulations have been performed in the same configuration unless specified otherwise

As is mentioned earlier, the QG flows supercritical w.r.t. baroclinic instability have been studied in much detail in the past. A well established method of predicting the growth rate of the instability is through linear analysis. Nevertheless we observed that there is a discrepancy in the growth rate as predicted from linear analysis and the one estimated from the nonlinear simulations. This is evident from the semilogarithmic plot of KE as a function of time depicted in Fig. 3.2a.

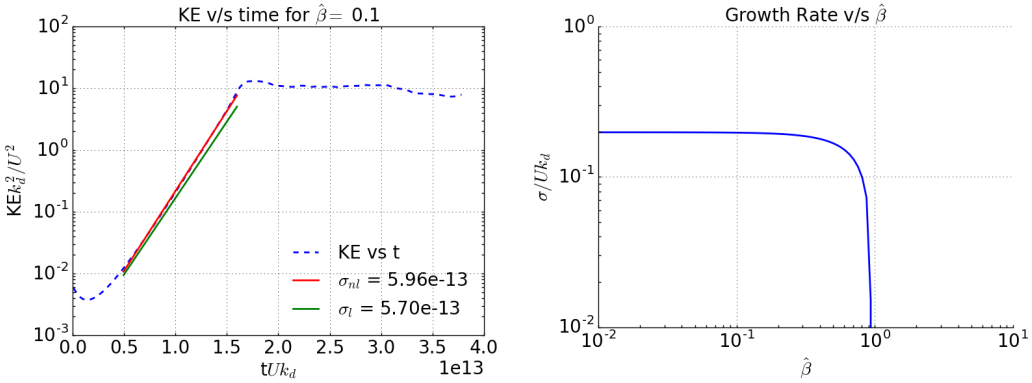

(a) KE as a function of time for $\hat{\beta} = 0.1$ (b) Growth rate as a function of $\hat{\beta}$ as predicted from linear analysis

Figure 3.2: Plots depicting deviation from linear behaviour

For baroclinic flows in the supercritical limit, initially, most of the energy of the perturbation is concentrated in a single mode but after a short while the flow becomes turbulent. It continues to remain in the turbulent state which can be inferred from the potential vorticity profile of the upper layer. There is also a certain isotropy in the energy spectrum. As we move towards the subcritical regime the mechanism for the evolution of the flow changed which is discussed in the upcoming section.

3.1 PV homogenisation and appearance of statistically steady states

As per the predictions form the linear analysis of QG flows, no instability exists when the flow is subcritical w.r.t to baroclinic instability, however the plot for KE as a function of time indicates that there indeed exists and instability. By looking at the evolution of the potential voriticity profile, we determined that the instability grows in a steady fashion, following which the flow becomes turbulent. Further, the PV profile homogenises and staircase like structures are obtained. This state of the flow is statistically steady and further evolution of the profile does not indicate any change.

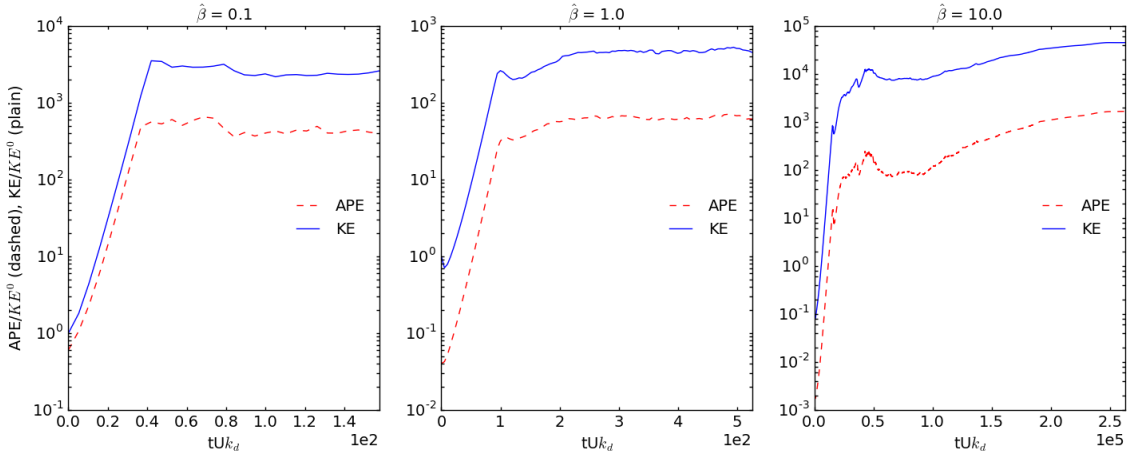

(a) Energy profiles for various $\hat{\beta}$

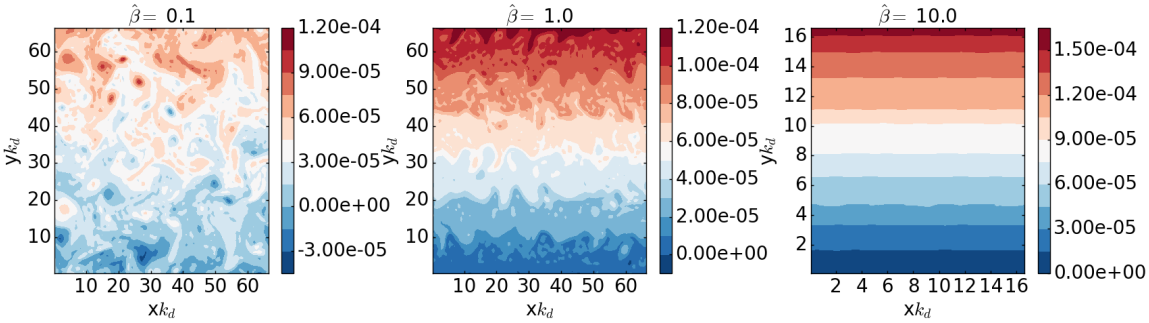

(b) Upper Layer PV profiles for various $\hat{\beta}$

Figure 3.3: Temporal evolution of total KE and total APE normalised w.r.t. to initial KE and the PV profiles for various flow regimes

By looking at the evolution of KE, one can say that a statistically steady state has been achieved as the KE does not fluctuate as a function of time after a steady state is obtained. Fig. 3.3a and Fig. 3.3b depict the temporal evolution of KE and the potential vorticity profile when a statistically steady state is achieved for various flow regimes.

We move to examining the energy spectrum for the subcritical limit. Fig. 3.4 depicts the temporal evolution of the energy spectrum for $\hat{\beta} = 4.0$. As is evident from the figure, upon stabilisation, there is an anisotropy in the energy spectrum and

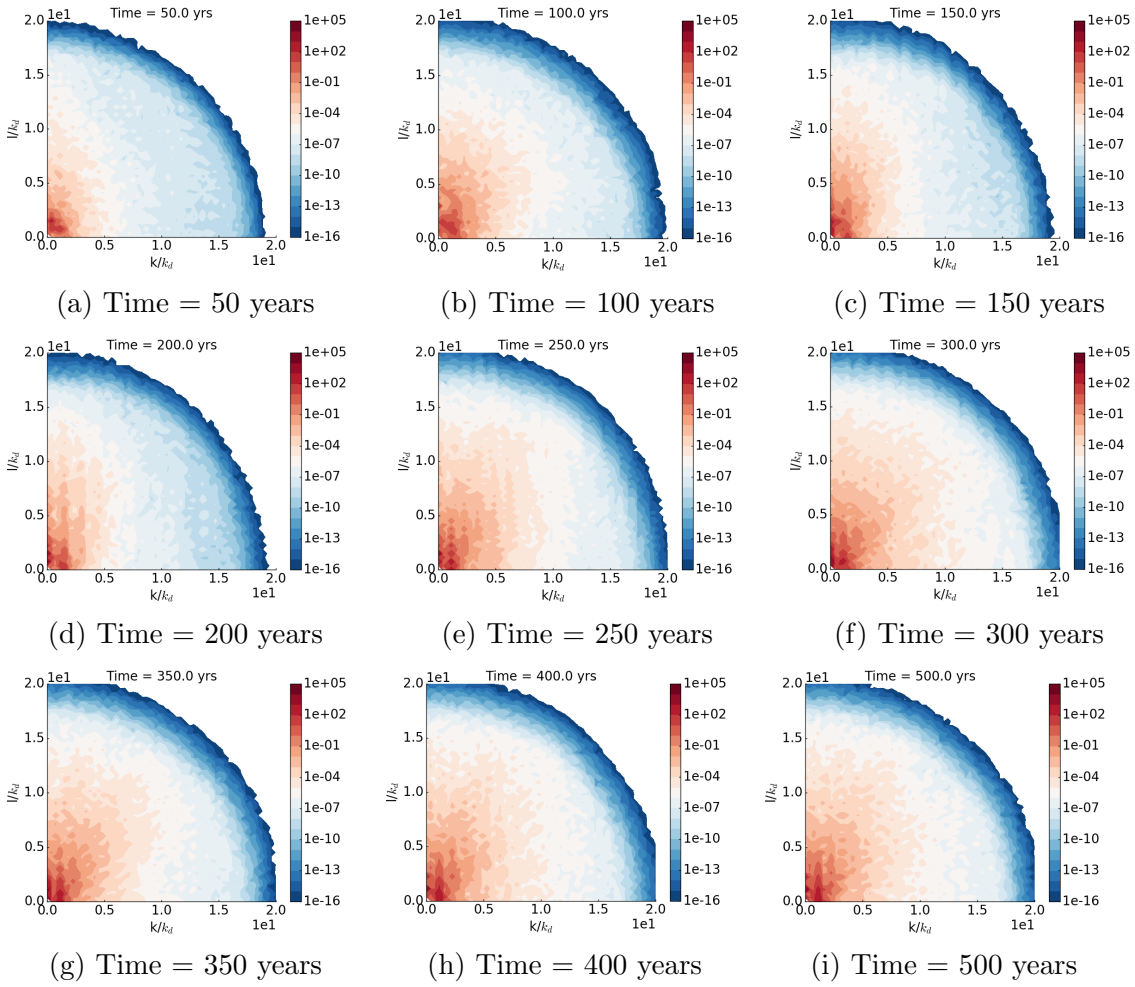

(a) Time = 50 years (b) Time = 100 years (c) Time = 150 years

(d) Time = 200 years (e) Time = 250 years (f) Time = 300 years

(g) Time = 350 years (h) Time = 400 years (i) Time = 500 years

Figure 3.4: Zonal anisotropy in the energy spectrum for $\hat{\beta} = 4.0$

considerable fraction of the energy is concentrated in the zonal modes.

We analyse the contribution of the zonal flows to the spectrum. The spectrum in the Fourier space is computed and the total energy (E_{tot}) is examined as a function of k for different values of $\hat{\beta}$. Rhines, in his celebrated article [11], proposed the k^{-5} scaling law [12] for the energy spectrum. However, recent studies have established that the proposed law is not universal, instead the scaling laws are for zonal spectrum have a dependence on the jet patterns [13]. Fig. 3.6a illustrates that the spectrum obtained in the vicinity of the $\hat{\beta} = 1$.

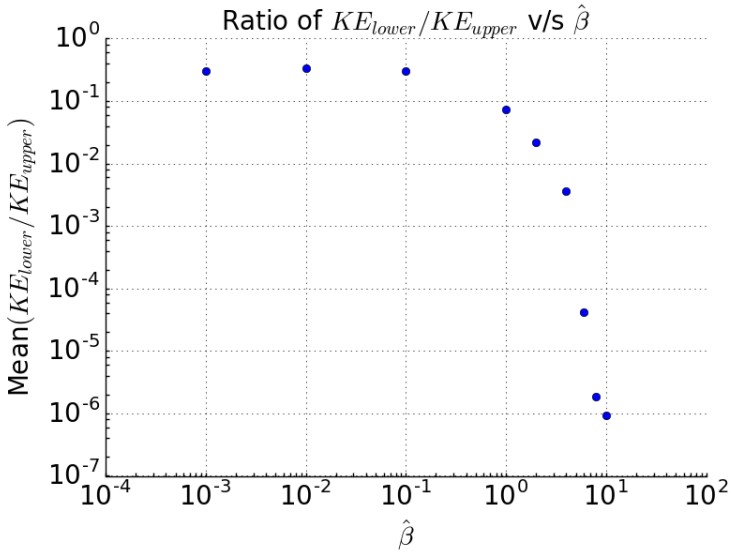

Figure 3.5: Average ratio of KE in the lower layer to upper layer as a function of $\hat{\beta}$

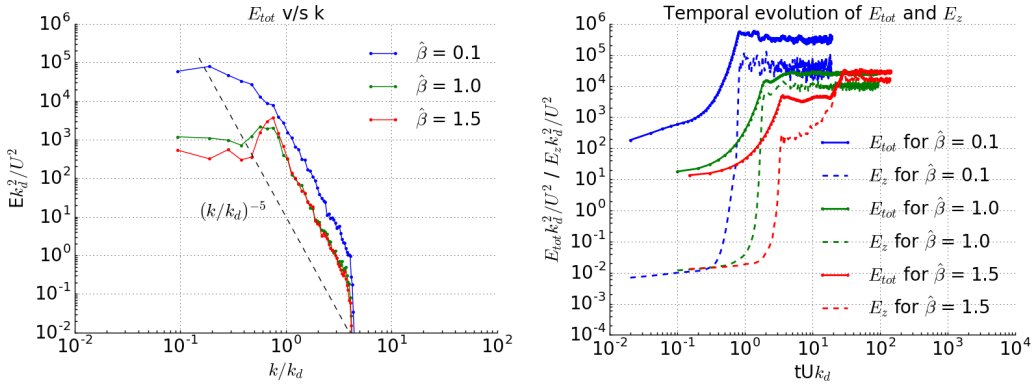

(a) Scaling behaviour of E_{tot} (b) Temporal evolution of E_z and E_{tot}

Figure 3.6: Scaling behaviour for E_{tot} profiles and temporal evolution of E_z and E_{tot}.

As has been mentioned, the PV staircase appears after the flow has stabilised and persists on further evolution. An evident difference between the statistically steady states and isotropic turbulence is that most of the energy for the statistically steady states is concentrated in the zonal modes. A quantitative parameter for identifying these states would be the ratio E_z/E_{tot}.

It's noteworthy that there is a rise in this ratio from $\hat{\beta} = 0.6$ onwards. This can

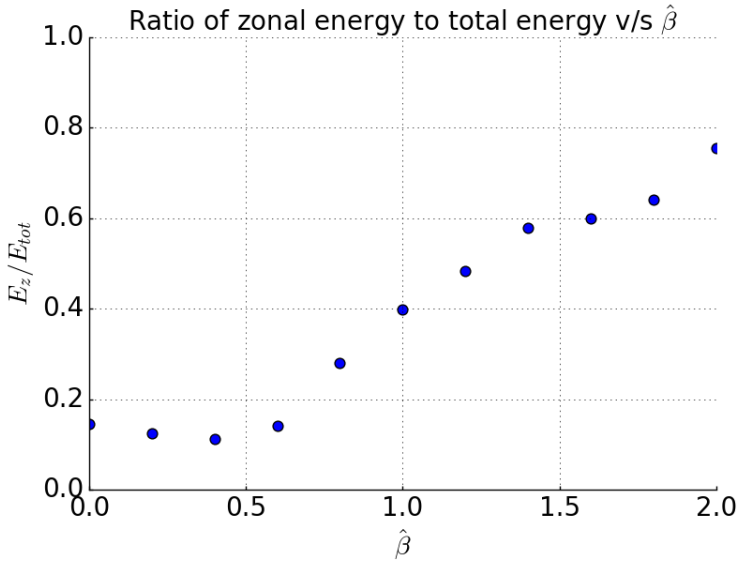

Figure 3.7: Ratio of zonal energy to total energy as a function of $\hat{\beta}$

be attributed to the fact that the staircase structures start to emerge from $\hat{\beta} = 0.6$ onwards but there is still some contribution from the vortex structures in the PV profile (refer to Figure 3.8). We now try and quantise the number of stairs obtained during the statistically steady state.

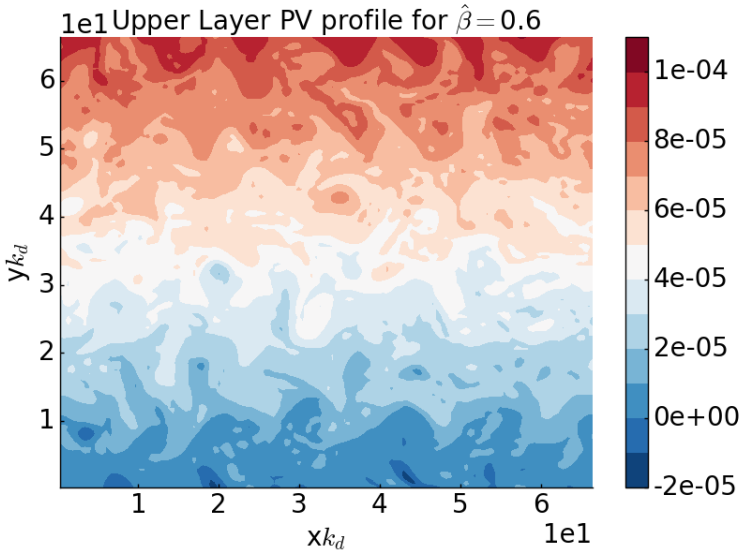

Figure 3.8: Upper layer PV profile for $\hat{\beta} = 0.6$

3.2 Counting the number of stairs

Rhines, in his study of turbulence in beta plane [11], also established the concept of wavenumbers of zonal jets (Rhine's scale).

$$k_{Rh} = k_\beta = \sqrt{\frac{\beta}{2U}} \tag{3.1}$$

Following this, there have been many studies paying close attention to

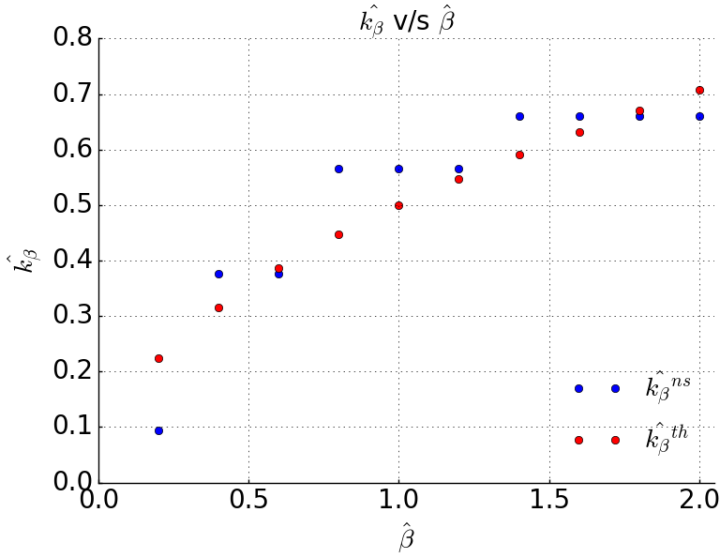

Figure 3.9: Rhines' scale as obtained from numerical simulations and theoretical values as a function of $\hat{\beta}$.

homogenisation of potential vorticity [14] and emergence of zonal jets.

As illustrated in Figure 3.3b, we observe such homogenisation for the subcritical domain. Multiple zonal jets appear in the PV profile and we have at our hands a PV staircase [15]. In this section we aim at counting the number of stairs as a function of $\hat{\beta}$. This can be done effectively by plotting $< \frac{\partial q}{\partial y} >$ as a function of y, where q is the PV. Due to the staircase like structure, there should be distinct spikes in this plot. These spikes are indicative of 'climbing a stair'. By counting the number of maximas (the number of spikes), we can determine the number of stairs as a function

of $\hat{\beta}$. A spike is only identified as a stair if the value of $< \frac{\partial q}{\partial y} >$ ($< a >$ indicates the average of a) exceeds $1/\sqrt{2}$ times the maximum value. This threshold is represented by the red line shown in Figure 3.10b. Using the method illustrated by Figure 3.10,

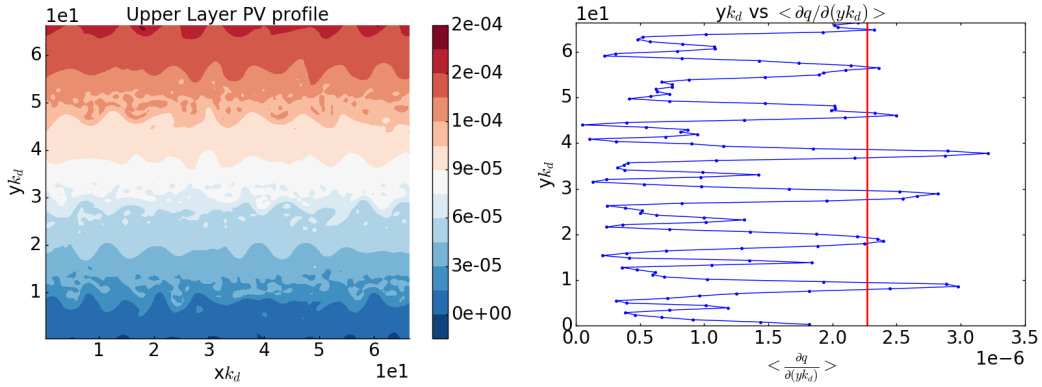

(a) Upper layer PV profile for $\hat{\beta} = 1.8$ (b) yk_d as a function of $\frac{\partial q}{\partial (yk_d)}$

Figure 3.10: Upper layer PV and yk_d as a function of $< \frac{\partial q}{\partial (yk_d)} >$ for $\hat{\beta} = 1.8$.

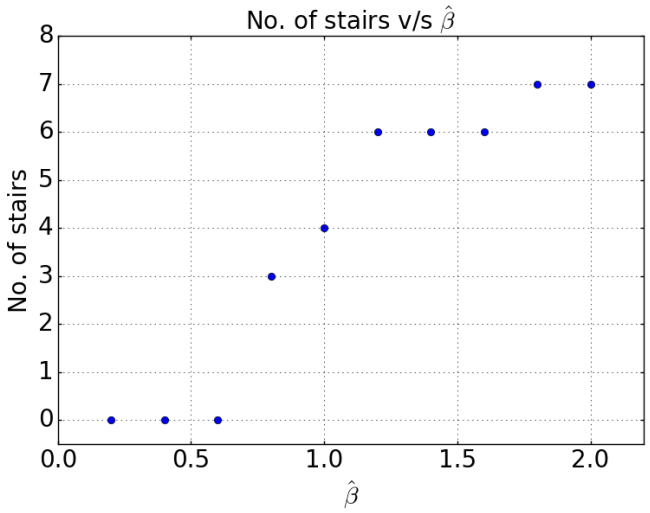

Figure 3.11: No. of stairs as a function of $\hat{\beta}$.

we estimated the number of stairs formed as a function of $\hat{\beta}$. Figure 3.11 illustrates these results. The formation of these PV staircases have been discussed in the next section.

3.3 PV staircase

Formation of zonal jets in the Earth's atmosphere, oceans and in the atmosphere of other planets, is a phenomena which has been known for a long time. The staircase like structure and the vortices visible on Jupiter have been studied extensively as well [16] and much has been debated over the formation of these zonal jets. During the course of our study, we observed similar jets originating in the PV profiles of the two-layer QG model lying in a β - channel. The organisation of the PV profiles into staircase like structures is of great interest and Dritschel and McIntyre [17] have made certain significant contribution in explaining these structures. In this section explores the possible reasons for formation of such structures in our model.

It is suspected that for the aforementioned model, the formation of these jets is due to the inhomogeneous sideways mixing of PV across the gradient. High values of $\hat{\beta}$ can be attributed to steeper meridional gradient of Coriolis force. This results in more dominant effects of rotation on the fluid which discourages the retention of vortex like structures formed in the PV profile thus eventually leading to formation of streamline jets.

The formation of these jets is also accompanied by a positive feedback mechanism which further encourages the persistence of the staircase like structure. The vortices experience a shear strain across the boundaries of these jets which acts as a barrier for the vortices to break through. The weak vortices aren't able to break through the barrier and diffuse in the mean flow, the stronger vortices which are able to break through the barrier eventually diffuse in the mean flow as well but result in the widening of the staircase. This positive feedback mechanism further sharpens the jets.

In the celebrated work by Rhines [11], he established that turbulence is necessarily

accompanied by waves which puts into picture the fact that radiation stress also might have something to do with the formation of the PV staircase. The radiation stress induces the currents which further encourage the jet like profile by helping retain the mean flow initially present.

We believe that this discussion provides an adequate understanding of the novel findings unveiled through the course of this study and also gives some unique insight into the problem undertaken.

Chapter 4

Conclusions

The study revealed many interesting characteristics of the subcritical baroclinic flow. We observed that in the subcritical regime, there is an instability which grows in the initial stages of the flow following which the flow becomes turbulent. It is noteworthy that this turbulence does not occur due to (linear) baroclinic instability. The flow then equilibrates and we register strong nonlinear reorganisation of the flow structures into staircases.

The staircase like structure was quantised and we found that the appearance of such PV staircases can be attributed high values of $\hat{\beta}$ implying a steeper meridional gradient and resulting in dominant effects of rotation accompanied by suitable positive feedback mechanism and wave turbulence. Also, in this regime, there is no barotropization which is in contrast with usual picture of geostrophic turbulence. The reason may be that we are in a regime of weak turbulence close to the one described by Harper et al. [18].

An extension of this work would be to see how the dynamics of the flow evolve when the domain aspect ratio is not unity. Also, it might be interesting to explore what effect does the increase in bottom friction have on the dynamics of the flow. Does the presence of higher dissipation have any impact on the staircase structure?

References

[1] Geoffrey K Vallis. *Atmospheric and oceanic fluid dynamics: fundamentals and large-scale circulation*. Cambridge University Press, 2006.

[2] Joseph Pedlosky. Finite-amplitude baroclinic waves. *Journal of the Atmospheric Sciences*, 27(1):15–30, 1970.

[3] Mankin Mak. Equilibration in nonlinear baroclinic instability. *Journal of the atmospheric sciences*, 42(24):2764–2782, 1985.

[4] BT Willcocks and JG Esler. Nonlinear baroclinic equilibration in the presence of ekman friction. *Journal of Physical Oceanography*, 42(2):225–242, 2012.

[5] Patrice Klein and Joseph Pedlosky. A numerical study of baroclinic instability at large supereriticality. *Journal of the atmospheric sciences*, 43(12):1243–1262, 1986.

[6] EO Holopainen. On the effect of friction in baroclinic waves[1]. *Tellus*, 13(3):363–367, 1961.

[7] Richard D Romea. The effects of friction and β on finite-amplitude baroclinic waves. *Journal of the Atmospheric Sciences*, 34(11):1689–1695, 1977.

[8] Joseph Pedlosky. *Geophysical fluid dynamics*. Springer Science & Business Media, 2013.

[9] Brian F Farrell and Petros J Ioannou. A theory for the statistical equilibrium energy spectrum and heat flux produced by transient baroclinic waves. *Journal of the atmospheric sciences*, 51(19):2685–2698, 1994.

[10] Shian-Jiann Lin and Raymond T Pierrehumbert. Does ekman friction suppress baroclinic instability? *Journal of the Atmospheric Sciences*, 45(20):2920–2933, 1988.

[11] Peter B Rhines. Waves and turbulence on a beta-plane. *Journal of Fluid Mechanics*, 69(03):417–443, 1975.

[12] Huei-Ping Huang, Boris Galperin, and Semion Sukoriansky. Anisotropic spectra in two-dimensional turbulence on the surface of a rotating sphere. *Physics of Fluids*, 13(1):225–240, 2001.

[13] Sergey Danilov and David Gurarie. Scaling, spectra and zonal jets in beta-plane turbulence. *Physics of fluids*, 16(7):2592–2603, 2004.

[14] Peter B Rhines and William R Young. Homogenization of potential vorticity in planetary gyres. *Journal of Fluid Mechanics*, 122:347–367, 1982.

[15] Colm Connaughton, Sergey Nazarenko, and Brenda Quinn. Rossby and drift wave turbulence and zonal flows: the charney–hasegawa–mima model and its extensions. *Physics Reports*, 604:1–71, 2015.

[16] Philip S Marcus. Jupiter's great red spot and other vortices. *Annual Review of Astronomy and Astrophysics*, 31(1):523–569, 1993.

[17] DG Dritschel and ME McIntyre. Multiple jets as pv staircases: the phillips effect and the resilience of eddy-transport barriers. *Journal of the Atmospheric Sciences*, 65(3):855–874, 2008.

[18] Katie L Harper, Sergey V Nazarenko, Sergey B Medvedev, and Colm Connaughton. Wave turbulence in the two-layer ocean model. *Journal of Fluid Mechanics*, 756:309–327, 2014.